

**Summary of activities undertaken in 2017 under the project
PN II–RU–TE–2014–4–1761: Intelligent Hierarchical Control of Distributed
Systems of Production and Use of Electricity**

In accordance with the project implementation plan, this step had four objectives:

1. Design of the bidirectional converter for energy transfer to/from the grid;
2. Design of the development system for the management of integrated energy production and use system;
3. Working/training visit;
4. Validation in physical environment of the management structure and algorithms for the integrated energy production and use system.

The activities corresponding to the four objectives are described in the table below:

	Objectives	Activities
2017 Single stage	Design of the bidirectional converter for energy transfer to/from the grid	Setting the structure and implementing the grid connection system (“Inverter/APF”)
	Design of the development system for the control of integrated energy production and use system	Setting the structure of the development system for the control of integrated energy production and use system
		Implementing and testing the development system
	Working/training visit	Working/training visit
	Validation in physical environment of the control structure and algorithms for the integrated energy production and use system	Implementing in physical environment the solution for the hierarchical control of the integrated system
Testing the solution for the hierarchical control of the integrated system using different scenarios regarding the random exogenous variables and setting the final parameters of the control structure		

The objectives set for 2017 have been fully achieved and all the activities in the implementation plan have been carried out. In the 2017 development stage, the dissemination results are as follows: 4 scientific papers presented at BDI indexed conferences (IEEE Xplore) (all pending ISI Proceedings indexing) and a doctoral thesis for which the PhD title was confirmed by the minister of National Education (Order 4097 of June 20, 2017).

**Objective I: Design of the bidirectional converter for
energy transfer to/from the grid**

1. Setting the structure and implementing the grid connection system (“Inverter/APF”)

The system connects to the grid via a connection point which also connects local consumers. The parallel active power filter includes control elements of the harmonic currents for each phase of the three-phase grid, as well as forced zero current in the neutral line route.

The hardware structure of the filter includes a voltage inverter with 4 active arms having IGBT power modules (100A, 1200V), and the control consists of four current control loops and an upper (slow) loop for voltage control inside the inverter.

Transducers have been provided for phase voltages, phase currents and neutral, as well as current transducers for the current injected by the active filter in the common point of coupling. In order to obtain the reference shape/curve of the current from the grid, transducers for phase voltage are used, whereas grid current transducers are used to implement current control loops. Current transducers connected to the output of the active filter are used only for monitoring the flow circulated by the filter in order to implement overload protection.

In the DC voltage area of the active power filter there is a voltage sensor and a current sensor used to implement the control loop of the internal voltage of the inverter.

The voltage inverter is connected to the grid by means of four inductances on ferromagnetic core.

The energy storage capacitor in the active power filter consists of a group of 470uF/450V serial-parallel capacitors, so that the working voltage can reach 700V, the required value of the correct operation of the current control loop.

The components generating electro-magnetic interference (air-gap inductance) and the condenser were assembled in a housing made of metal (iron).

The voltage control loop is based on a P-controller (proportional), without integrated component, to eliminate excess voltage caused by the disconnection of consumers (an intrinsic characteristic of the control strategy required for the operation of the active filter). A stationary error of up to 10% is acceptable both for the operation of the current control loops and for extracting information necessary for calculating the amplitude of the minimum current in the grid.

The electronic module for the implementation of the current loop (physically achieved: 4 modules - 3 phases + neutral) is based on a microprocessor type DSPIC33FJ128MC804 for switching applications. This module receives analog information from current and voltage transducers in the grid coupling point, as well as information about the voltage regulating error of the capacitor. According to the strategy of active filter control, the grid voltage curve (if the voltage is distorted, the sinusoidal form can be restored with a PLL loop) is multiplied mathematically with the voltage error on the DC voltage capacitor of the inverter, and thus provides the reference current for each phase of the grid. Zero value of the current is required for the ground wire, regardless of time.

The electronic module for the implementation of the voltage loop includes voltage and current transducers for the DC voltage of the inverter, as well as a microcontroller type DSPIC33FJ128MC804 for the implementation of the voltage regulator.

The electronic module for signal acquisition in the common grid connection point integrates components from the common grid connection point: current transducers on each phase and neutral, voltage transducers between each phase and neutral, current transducers circulated through each arm of the active power filter. The compact structure ensures minimal electromagnetic interference between high current lines and transducers outputs of small signal. For each transducer two outputs were provided, one in the 0-3,3V range - to use the analog input signal of DSPIC processors, and one in the -10V, + 10V range, to display the signal on the computer through analog inputs of the numerical acquisition system dSpace DS1103.

The inductances necessary for the connection of the active power filter to the grid represented the most challenging technological achievement. The solution adopted was to use ready-made inductors on iron core with transformer sheets, so that the losses caused by switching the inverter to a 20 kHz frequency be as small as possible.

2. Implementing control loops in the active filter/inverter

The active power filter operates independently of the computing system on the setup, based on its own control loops implemented in the local digital processors. The processor operating frequency of the active power filter is 80MHz, and each instruction executes in 2 periods of the clock signal. The software was written in Mikropascal.

For alternative signal acquisition, since the input domain of the analog-digital converter is between 0 and 3,3V, the analog signal is centered on 1,5V. At processor initialization, a function was implemented by which the offset value of the analog signal is accurately measured and then extracted from the resulting numerical value at the end of each conversion.

The voltage control loop is realized in an infinite, slow loop:

```
while 1 do
  begin
    // voltage value on the capacitor
    tmp1_longint:=UDC;
```

```

//voltage error on the capacitor
//tmp2_longint:=3*UR_redresat-tmp1_longint;
tmp2_longint:=1100-tmp1_longint; //650Vcc
// KP KI constants for voltage regulator
tmp2_longint:=4*tmp2_longint;
if tmp2_longint>1000 then tmp2_longint:=1000;
errUDC:=integer(tmp2_longint);
pwm_set(2047-errUDC); //value centered on 50% to also operate for grid injection
value_dislay();
end;

```

The current control loop is realized within a real-time interruption activated by a 20 kHz frequency, simultaneously with the PWM signal generated at control output.

To operate as voltage inverter, the current control loop is replaced with a loop for generating a PWM signal with a variable duty cycle by a sinusoidal law.

3. Checking the operation of the voltage inverter as parallel active power filter

For a single-phase load type bridge rectifier with RC output, the following waveforms have been acquired (Figure I.1): channel 1 of the oscilloscope = phase voltage (230Vac); channel 2 of the oscilloscope = load current (5A peak). The spectrum of the current waveform is shown in Figure I.1b.

After activation of the active power filter, the same signals show as in Figure I.2. It can be noted that the form of the grid current has become almost sinusoidal and the amplitude decreased. The consumption of the active power filter is given by the switching losses on each arm of the inverter. The switching frequency is 20kHz and is at the recommended upper limit for the IGBT modules used.

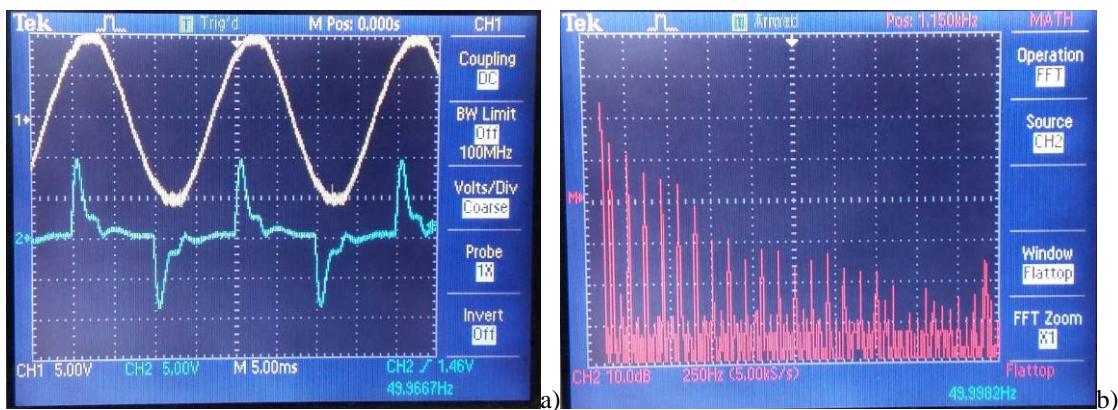


Fig. I.1. Rectifier bridge load with RC output – active power filter stopped: a) CH 1- phase voltage, CH 2- input current; b) input/load current spectrum

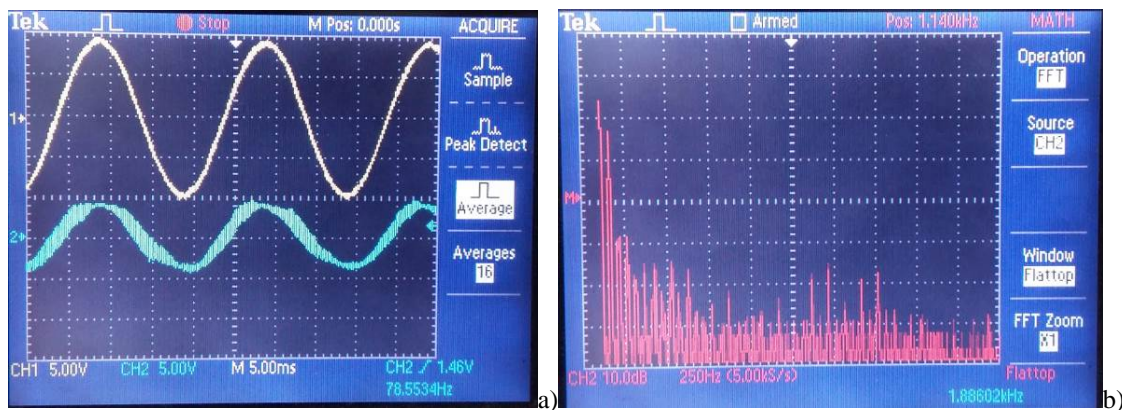


Fig. I.2. Rectifier bridge load with RC output – active power filter activated: a) CH 1- phase voltage, CH 2- input current; b) input/load current spectrum

When the consumer rectifier bridge with RC load is connected with a resistive load of 400 W (hotplates), the following were acquired: phase voltage and current (Figure I.3a), and after the activation of the active power filter (APF), the current has become as shown in Figure I.3b.

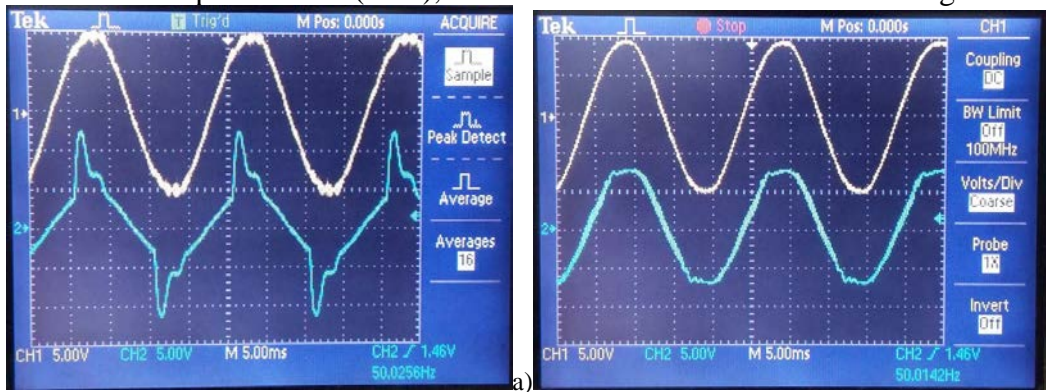


Fig. I.3. Rectifier bridge load with RC output and 400W resistive load: a) active power filter stopped: CH 1 – phase voltage, CH 2- load current; b) active power filter activated: CH 1 – phase voltage, CH 2- load current

The following results highlight the operation of the active power filter in inverter mode. In order to supply local consumers by means of the active power filter, a DC voltage was injected in the continuous voltage capacitor of the voltage inverter. Prior to injection, the waveform of the current phase of the grid was as shown in Figure I.4a. After connecting the current source to the active filter, the amplitude of the grid current has become almost zero (Figure I.4b). From the energy balance between the filter, the consumer, the auxiliary current source and the grid, the grid current can be in phase with the grid voltage, zero or out of phase. The neutral grid current with consumer in operating mode means supplying the consumer from the auxiliary current source by means of the active power filter.

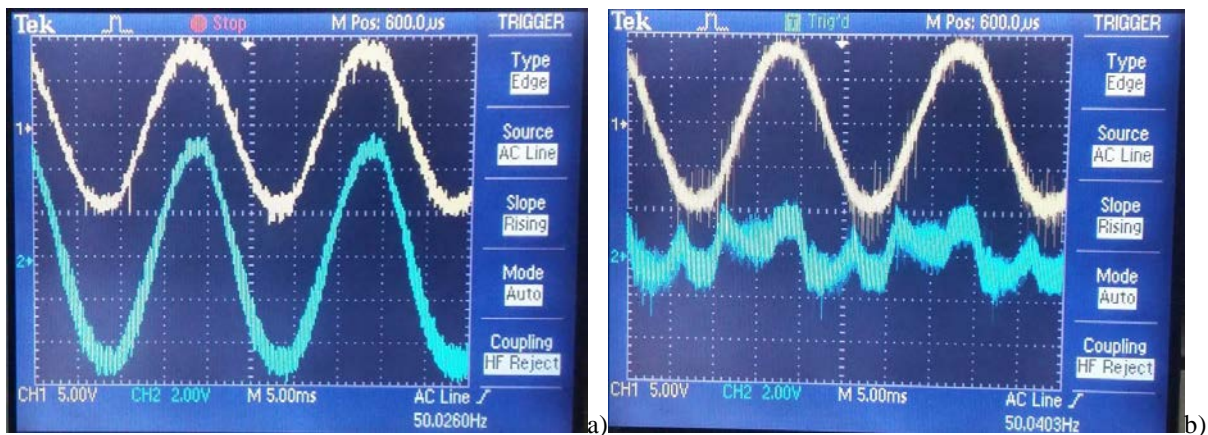


Fig. I.4. a) operating the active filter in compensation mode; b) operating the active filter in inverter mode

In conclusion, it has been demonstrated that the equipment developed in the project can function both in inverter mode and in active power filter (APF) mode. This way, the management of the energy flow from/to the grid or the compensation of disturbances and reactive power are possible.

Objective II: Design of the development system for the control of integrated energy production and use system

1. Setting the structure of the development system for the control of integrated energy production and use system

1.1. Choosing topology and configuring DC/DC converters for renewable energy conversion

The modifications made to DC/DC converters, as compared with the versions in the *Scientific Report on the 2016 stage*, are presented below.

Establishing topology takes into account input and output voltage levels, the necessary galvanic insulation and a common connection between the input and the output. To extract maximum power from the PV source, a *boost* circuit can be used; for the wind power supply, a *buck-boost* is needed, H-bridge with transformer or SEPIC. The SEPIC configuration was selected because of the similarities with the *boost* circuit of the power connections of the electrical components.

The disadvantage of the SEPIC topology is that the voltage at the static switch current Q1 and the current through Q1 will achieve, by design, the sum of input and output values without taking into consideration any transient events. For this reason, IGBTs were used for the SEPIC, and MOSFETs for boost.

Galvanic isolation between power and control circuits was not used; voltage measurement was made with a resistive divider and current acquisition was made with ACS758-100U specialized transducers with Hall effect. All transducers are accompanied by *low pass* filters and voltage level converters. For the user interface a small area has been allocated in the outer side of the processing box, with buttons, LEDs, and BNC connectors for acquisition of voltage and currents by means of the dSpace control board. A graphical display is connected to monitor the internal variables. All the signals that lead to BNC connectors are screened and the screen is connected to the same point on the circuit board. As the external interface is insulated from the metal housing, no ground loop was created.

The coils used in DC/DC converters were made on Epcos ETD59, N97 ferrite core. For the *boost* converter (converter dedicated to PV), each inductor is made of 1,8 mm copper conductor, resulting in 2,4mH. For each core a 1,6 mm air gap was placed to prevent saturation at high currents. For the SEPIC converter (dedicated to wind power), both coils for a converter arm are made on the same magnetic core, on the opposite ends of the bobbin support. Also, the air gap was 1,6 mm. The inductance of each coil is about 0,6mH.

The *control loops* of the converter are implemented in a 16-bit processor of general use, in the family of dsPIC33F, able to generate alternative PWM signals, due to the Capture/Compare/PWM internal module. The following control methods have been implemented:

- the scanning of the duty-cycle (*duty-cycle sweep*) followed by a jump to the value that offered maximum input power (Figure II.1.11). The method is useful for PV or any other source that supports fast load variations from zero to 100% and it will find the point of maximum power no matter how many local maxima exist;
- the classical algorithm *perturb and observe*, enhanced with a second loop to find the minimal useful disturbance for both PV and wind applications. Using this algorithm for a wind turbine produced poor results because control loops must act slower than the response time given by the inertia of the generator and the blades;
- the simplified incremental conductance (IC) method;
- *proportional* controller where the filling factor follows the input voltage. This method provided the best results for the wind turbine, since output voltage of the turbine is proportional to angular velocity of the rotor. The relationship between the duty-cycle and the power output is not linear, so that the entire feature was divided into smaller segments, and the coefficient P was determined experimentally for each;
- *PWM modulator with reference received from an external source* (for example, the dSpace acquisition and control board). This feature allows the implementation of any control algorithm outside the digital processor and the use of the DC-DC converter circuit only for DC switching.

1.2. Establishing the structure of the PV emulator

For the PV emulator necessary to achieve project objectives, following a technical and economic analysis, a programmable voltage source and a DC/DC converter were preferred, together with a control algorithm.

The experimental platform for the testing of the PV emulator includes the following equipment: programmable voltage source, DC/DC converter with integrated MPPT algorithm, battery pack, resistive load, PC with data acquisition board and DS1103 controller board, PX4 junction box, Matlab and ControlDesk softwares.

The programmable voltage source type Magna Power SL32-46/230+HS can generate current-voltage profiles as they are found at the output of the photovoltaic panels. Source parameters can be configured by a computer using USB or Ethernet interface via a dedicated application. The source may be programmed for a wide range of current-voltage profiles. The coordinates of the profiles can be modified manually to emulate the characteristics of the desired photovoltaic panel. The application adjusts the characteristics emulated given the required environmental conditions - light and temperature. The source can work in power source or voltage source modes.

Nominal output parameters are 32V and 46A, which are also the limits imposed by the source for emulating photovoltaic characteristics. With reference to PV parameters commonly commercially available, with SL32/46 programmable voltage source may be emulated, for example, a group of five panels connected in parallel, each having 35 cells in series (ex. KC130TM). In this case, the voltage will be 17,6V and the current 37A at the point of maximum power. The amplitude of the short-circuit current for this panel system is 40A, close to the maximum 46A allowed by the programmable source. This way, the maximum power of the emulated system is about 650W. The maximum power emulated can be increased by using the characteristics of some commercial panels adequate to the source, which are not, nevertheless, common.

The DC/DC converter provides the interface between the emulated photovoltaic source and the DC distribution (DC bars). Its structure is classic: *boost* converter with 4 levels connected in parallel. Using this structure can reduce the gauge of the converter, as less powerful components are employed, available at lower prices, the characteristics of which are closer to the ideal (low resistivity, inductance realized by a smaller section conductor, higher switching frequency), and the switching frequency of the converter is four times higher (40 kHz) than that of individual floors (10 kHz). Limit parameters: unidirectional current transducers 0-100, MOSFET 50A/150V transistors, ultrafast 20A/200V diodes.

A first version of the converter included IGBT power transistors, structured on separate modules (power module, control module, transducer modules) to make testing and circuit changes easy. After the first set of tests and structure validation, the *boost chopper* was restored and enhanced. The final version preserved the conversion structure initially proposed, but IGBT transistors were replaced by MOSFET transistors to reduce power losses at switching. Also, the entire converter was made in a compact form, on the same circuit board, together with all the components of the above-mentioned power electronic circuit: the power, the control and the transducers (Figure II.1).

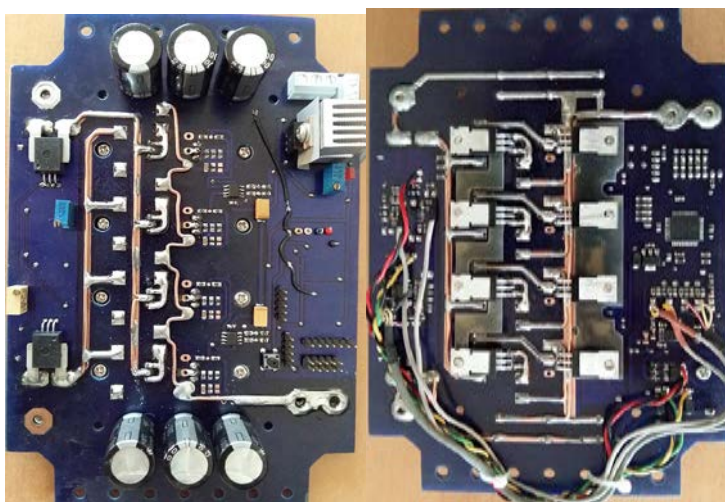


Fig. II.1. Power electronic circuit, face (left) and back (right)

Three control methods were implemented: *Perturb&Observe*, another method tested and implemented consists in determining the maximum power point by the method of testing the complete range of operating points (*Sweep*), and the third method was the *incremental conductance* method.

In these conditions, for the boost converter MOSFETs IPP200N15N3 were used with $R_{DS_ON} = 0,02 \Omega$ and $V_{DS} = 150 \text{ V}$, and IGBTs IRG4PC40FU with $V_{CES} = 600\text{V}$ and $V_{CE_ON} = 1,5 \text{ V}$ at $I_C = 27\text{A}$ were placed in the SEPIC circuit.

The circuit was implemented in two versions, one for the PV system, for which the boost configuration was chosen and one for the wind turbine generator, with SEPIC configuration. The same design of the circuit board was used, with differences only for the power components used.

The testing system was monitored with the software ControlDesk. Figure II.3 shows voltage and current curves during one of the experiments.

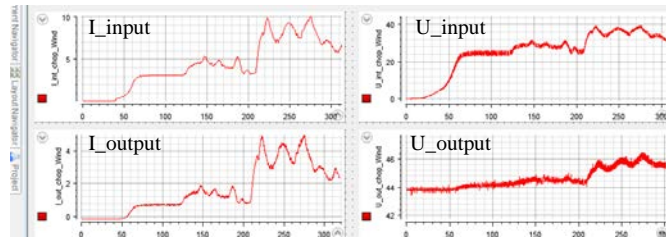


Fig. II.3. ControlDesk screen for DC/DC converter monitoring

2.2. Implementing and testing the PV emulator

The testing of the PV emulator was done in two successive steps aimed at validating the structure proposed for the *chopper boost*, the MPPT control and the structure of the emulator as a whole.

The first stage consisted in testing the *boost converter* realized in modular version, with IGBTs and MPPT control. In this stage, two sets of tests were made with two different power sources: a two-panel photovoltaic system ENGOTEC W1200-125 and a photovoltaic source emulator of 5 DC voltage sources. In **the second stage**, the tests were carried out on the final structure of the emulator. The *hardware* used to carry out the tests includes a programmable voltage source, the *boost converter* (version with MOSFETs) and the load as battery pack and a resistive component in two steps: 6Ω , 3Ω . The *software* of the emulator has two components: one that allows generating characteristic curves of the PV panel, supplied by the provider of the programmable voltage source, and the control component of the DC/DC converter that includes the MPPT algorithm.

In addition, to acquire relevant quantities, there have been used the *datalogger* of the programmable voltage source and the data acquisition structure corresponding to the stand developed within the project, consisting of: acquisition board and control dSPACE DS1103, current transducers and voltage interface software ControlDesk. This allowed comparison and validation of results.

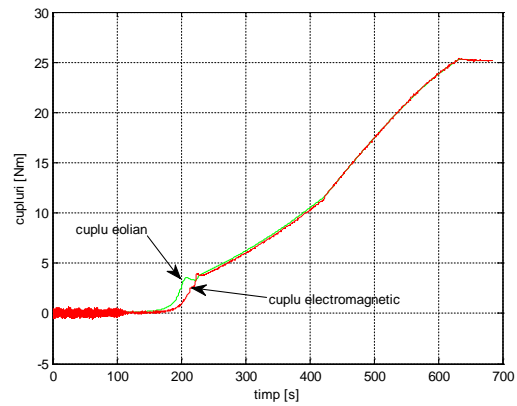
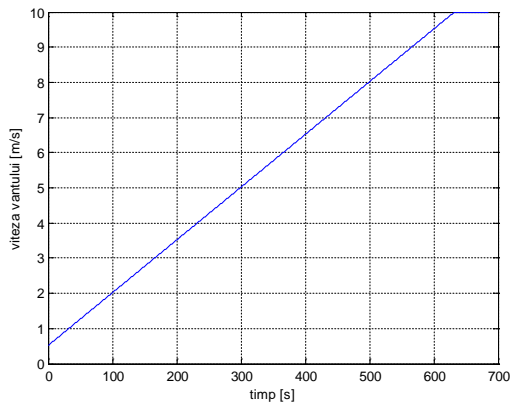
In order to obtain optimal energy conversion, the injection of power in the local DC grid is controlled by the DC/DC converter by means of the MPPT algorithm. In comparison with the use of real PV panels, the emulator brings additional challenges the most important of which is the interaction between the MPPT loop of the converter and the control subsystem of the programmable voltage source.

A first observation is related to the response time. In general, to have low ripple voltage, high capacity electrolytic capacitors and discharge resistors to maintain the output voltage when the source is empty are at the output of the programmable voltage sources. Although this is common for industrial applications, in case of a PV emulator it is necessary that the values of such components be smaller to allow using faster MPPT algorithms. For this reason, for the experimental stand the HS variant of the source was set. The advantage is given by the response time of 8 ms and the bandwidth of 45 Hz, compared with 100 ms and 2 Hz for the standard variant. The disadvantage of the HS version is the increase of the ripple voltage to 1,4Vrms compared with 40mVrms version without HS.

2.3. Implementing and testing the physical simulator for wind turbine

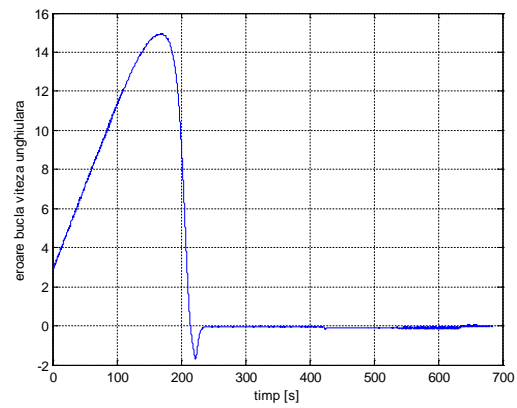
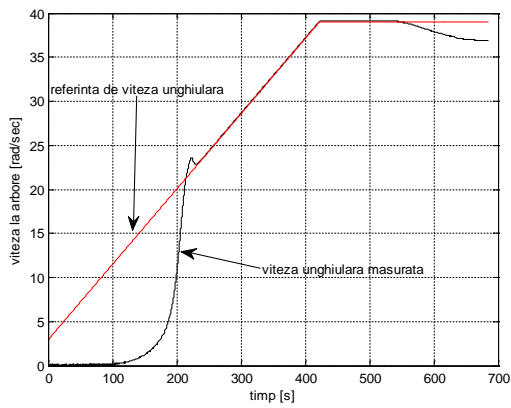
Three control methods have been implemented: P&O, IC (incremental conductance) (both of them with local control), and a third method consisting in the use of controllers implemented by the software Matlab/Simulink.

Figure II.6 shows the results for the stability of the wind system in its transition from zone 2 (optimization of wind energy conversion) to zone 3 (power limitation). A ramp-up wind speed profile was used with limitation to 10 m/s. At time $t=200s$ connecting the optimization loop, the control goes to value 2, the specific speed (λ) reaches the optimum value, $\lambda_{opt} = 7$, the coefficient of maximum power ($c_{pmax} = 0.476$), which means that the shaft rotational speed follows the optimum speed, as shown in Figures II.6c and II.6d, in the latter being represented the evolution of the optimization loop error. Figure II.6d shows that at time $t=420$ seconds, the optimization zone with shaft speed limitation is accessed. For this area, the optimization of wind energy conversion continues, and the extracted power continues to increase with the wind speed. At time $t=520$ seconds, power reaches 400 W (imposed as rated power), and the power limiting control loop is activated, managing to limit power value, even if the wind speed continues to increase.



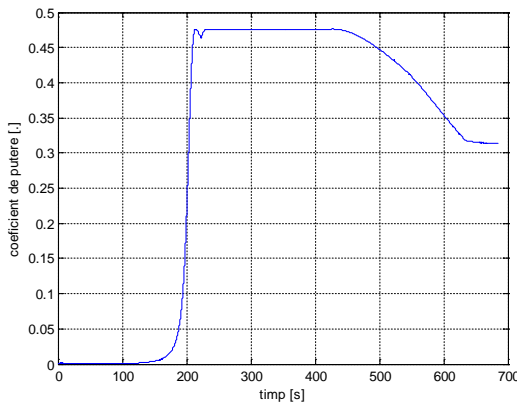
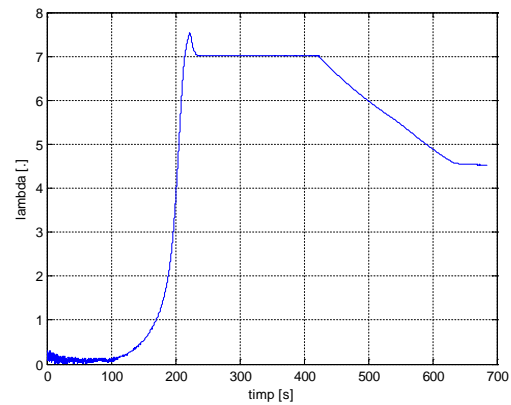
a)

b)



c)

d)



e)

f)

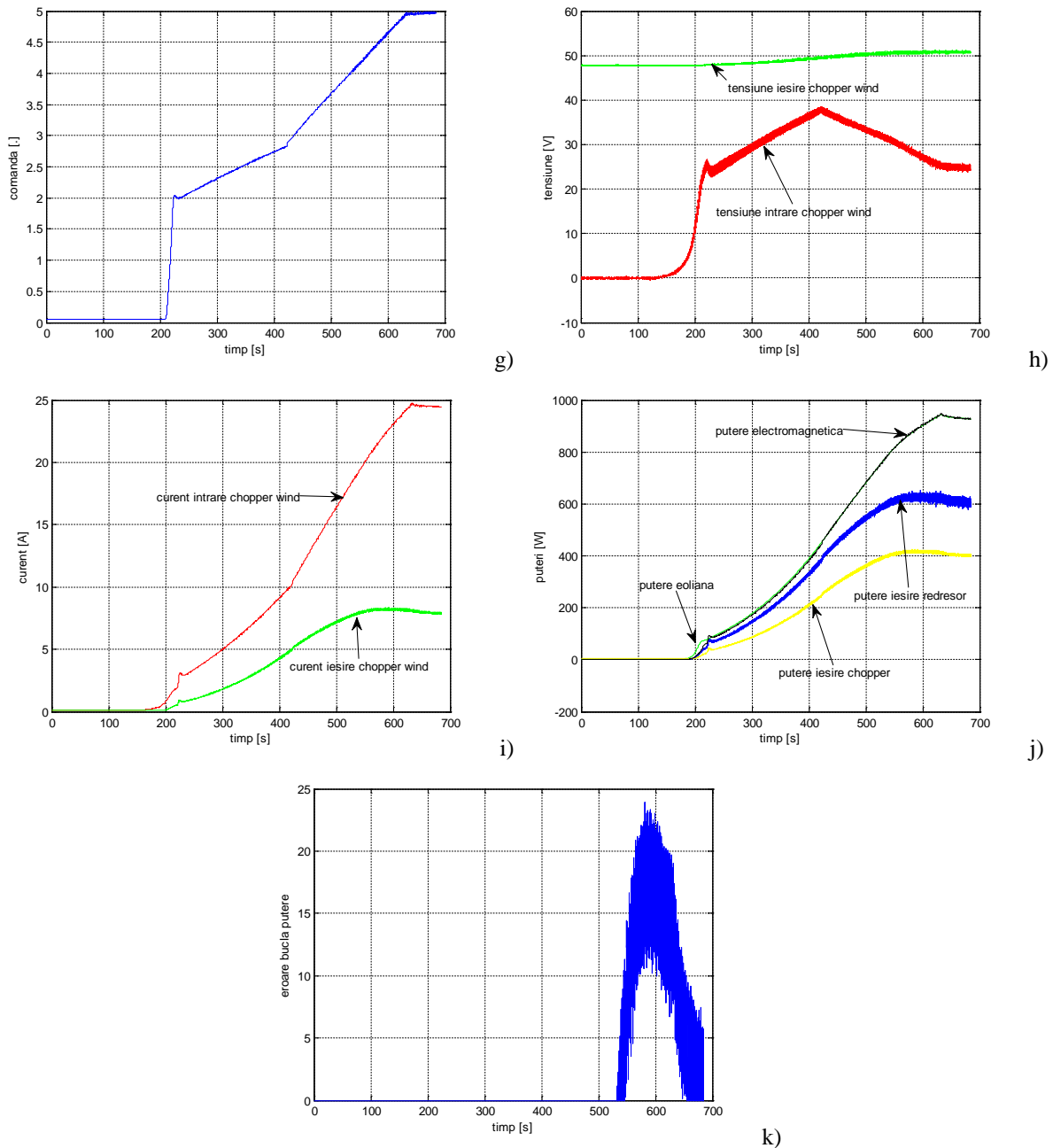


Fig. II.6. Evolution of main values of the wind turbine electro-mechanical simulator, in case of transition from zone 2 to zone 3, operating on battery and resistive load, with ramp-up wind speed profile

Power limitation through the *stall* effect can be also seen in the evolution of power coefficient (Fig II.6f) and specific speed (Figure II.6e), both values decreasing.

Moreover, the operation of the low-power distributed system was also tested for the case when the two renewable energy sources debit simultaneously, supplying AC consumers in insular mode. The results obtained showed that when the distributed system of production and use of energy from renewable sources works in autonomous operation mode, the priority is consumer supply, and battery life cannot be imposed as a priority by controlling the number of charging/discharging. A reliable solution may be to use a power source such as a diesel generator (to provide continuity of supply) or to connect to the national power grid.

Objective III: Working/Training visit

Ciprian Vlad, project team member, participated in a training organized by the German company dSPACE, in Paderborn, 12-13 September 2017. The aim of the training, “ControlDesk Basic and Advanced”, was to get trainees familiar with the dedicated computing environment

ControlDesk, given the fact that the entire automation platform of the distributed system of energy production and use is based on dSPACE structures that have the computing environment ControlDesk as software interface for process monitoring and control.

The content of the training focused on the following aspects: Installation; Introduction to CDNG; CDNG Project Management; Instrumentation; Data Measurement; Data Recording; Data Set Handling; Bus Navigator; Calculated Variables; Advanced Measurement and Recording; Signal Editor; Tool Automation and Event Handling.

Objective IV: Validation in physical environment of the control structure and algorithms for the integrated energy production and use system

1. Implementing in physical environment the solution for the hierarchical control of the integrated system

This activity aimed to implement the hierarchical control solution for the integrated system, on two levels:

- at lower level, control solutions have been implemented for the components of the system. For the wind system, a control solution was implemented which ensures the functioning on the curve between the points of maximum power (CRO) in zone 2 of the partial load characteristic, and, for limiting the power in zone 3, a system was implemented for controlling the power by bringing the turbine in *stall mode*, based on angular speed reduction when the wind speed increases. For the photovoltaic system, a control solution was implemented which ensures maximum power extraction. For the inverter/active power filter (APF), a control system was implemented that achieves the inverter/ PWM rectifier regime, ensuring output voltage and the power quality requirements imposed by the active power filter. Compared with the structure planned in the *Scientific Report on the 2016 stage*, for the final variant of the experimental setup, the option was for the separation of energy conversion paths for battery charge/discharge. Charging the battery from the grid is done via an autonomous rectifier with limitation of current and energy transfer from the battery to the consumers or the grid is done by injecting electricity into the DC voltage component of the voltage inverter used as active power filter.

The final control solution at a lower level implemented in physical environment uses a ControlDesk/dSpace computing environment for the wind system, the other elements using local software solutions.

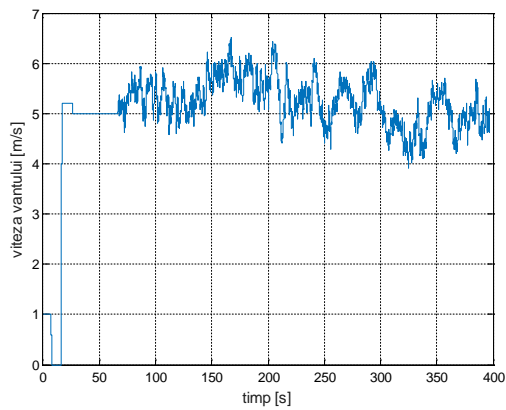
- at upper level, two control solutions were implemented to ensure the two components essential for the integrated system management: reducing energy transfer from the grid to the local network, and ensuring that requirements for increased battery life.

Considering the results of the simulation, the first control solution consists in using a controller with dead zone and hysteresis, for which the control outside the dead zone (positive or negative) is proportional to the control error. The second control solution uses a special controller, with a dead zone type three-phase block, performed by fuzzy techniques. Unlike the three-phase controller, the control outside the dead zone (positive or negative) is proportional to the control error. At upper level, the solutions implemented use ControlDesk computing environment based on acquisition boards dSpace DS1103. The control structures have been implemented as Simulink schemes that are compiled and loaded on the DS1103 dSpace board for running in real time.

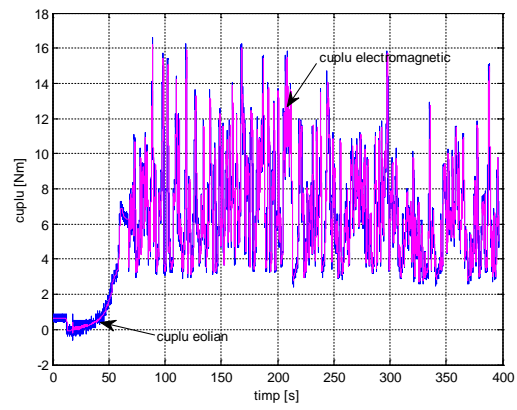
2. Testing the solution for the hierarchical control of the integrated system using different scenarios regarding the random exogenous variables and setting the final parameters of the control structure

Figure IV.1 shows the evolutions of the main features of the integrated energy production and use system when the two renewable energy sources debit and the battery, the national grid and the single-phase AC consumers are connected. In this case, the upper-level control structure resides in the use of a bipositional controller with hysteresis.

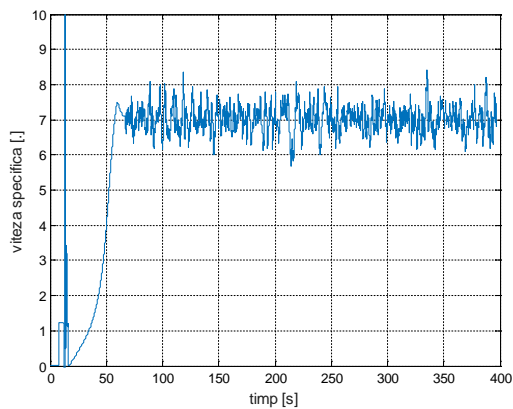
Figure IV.1a shows the experimental wind profile (a random profile for average speed value of 5 m/s). Figure IV.1b shows the wind torque and electromagnetic torque. Figures IV.1c and d show the evolution of specific speed and, respectively, power coefficient, and it can be noted that the adjustment of wind energy conversion into electricity is maximum, the specific speed presenting small variations around the optimum value (7), and the power coefficient evolving in the same direction around the maximum value (0,476). This can also be demonstrated by the evolution of the shaft rotational speed and of the angular speed loop reference, as shown in Figure IV.1e. Figure IV.1f shows the input voltage on the chopper for the PV emulator, the input voltage on the chopper for the wind turbine electro-mechanical simulator and the voltage on the DC line, where the two renewable energy sources supplies, the battery and the national grid are connected, and which can help in charging the battery and/or providing power for single-phase consumers when the renewable sources do not supply the necessary energy. It can be noted that, at this wind speed, the converters for the renewable sources increase the voltage and the battery voltage has variations around 48V.



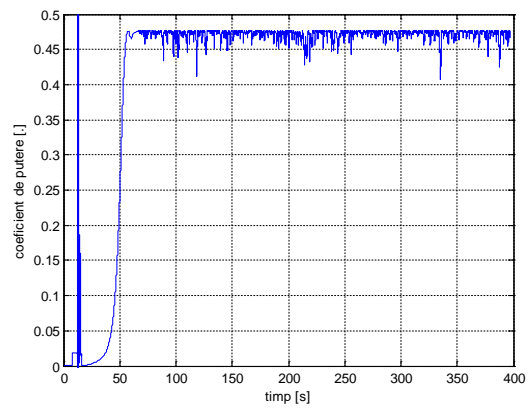
a)



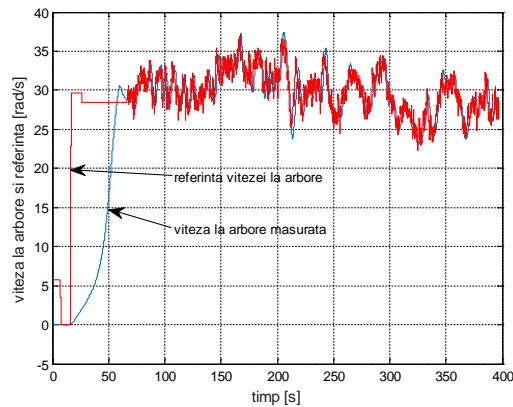
b)



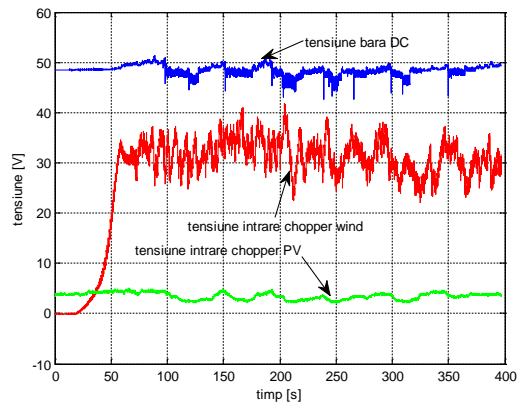
c)



d)



e)



f)

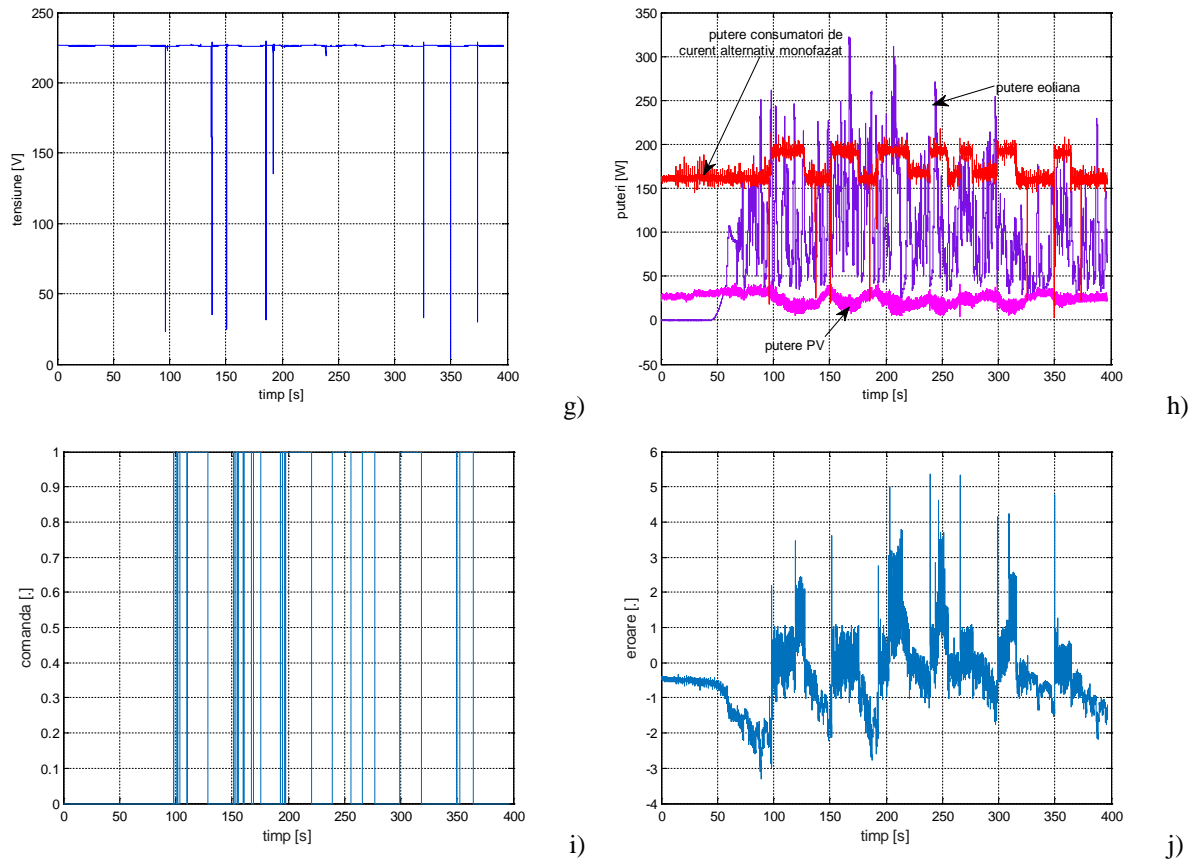
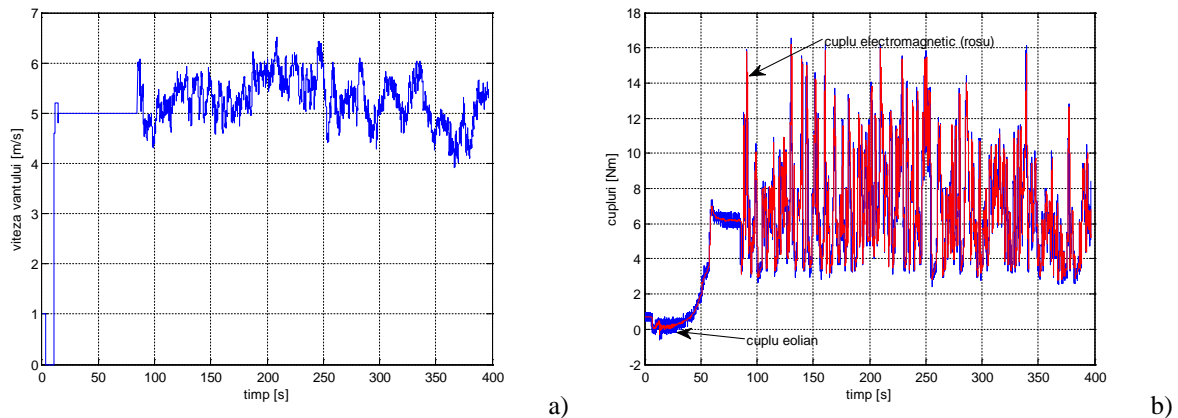
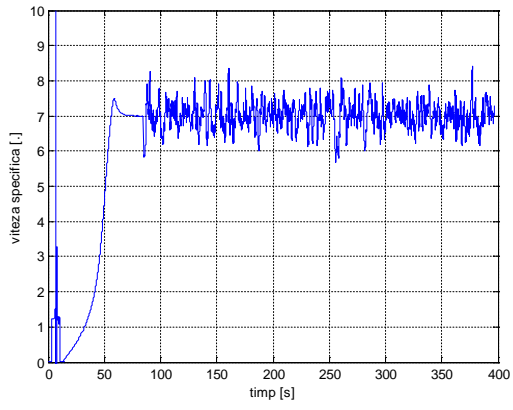


Fig. IV.1. Evolution of main features of the integrated energy production and use system when the two renewable sources debit, the battery, the mono-phase AC consumers and the national grid are connected, with on-off controller with hysteresis

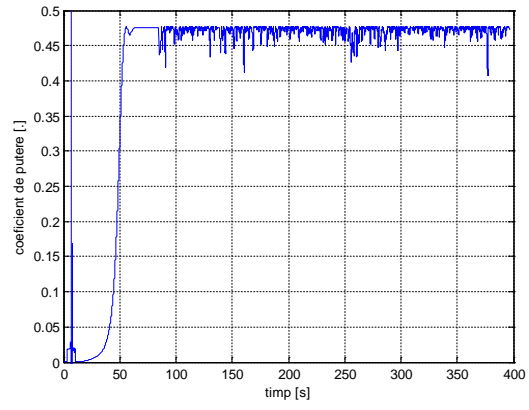
The voltage for single-phase consumers is represented in Figure IV.1g, and the power of the two renewable sources and of single-phase consumers are represented in Figure IV.1h. Figure IV.1j shows a good control result when the voltage reference on the battery was 48V. This comes with an associated cost regarding the frequent charge/discharge commutations, as shown in Figure IV.1i. Figure IV.2 presents the evolution of the major features of the integrated energy production and use system when the two renewable energy sources debit, and the battery, the national grid and the single-phase AC consumers are connected.

The upper-level control structure resides, in this case, in the use of a fuzzy controller. The evolution of the features represented are in the sense of those in the previous figures. Figure IV. 2 shows: a) the wind speed profile; b) the wind torque and the electromagnetic torque; c) the specific speed; d) the power coefficient; e) the shaft rotational speed and the optimization loop reference of the wind energy conversion into electricity.

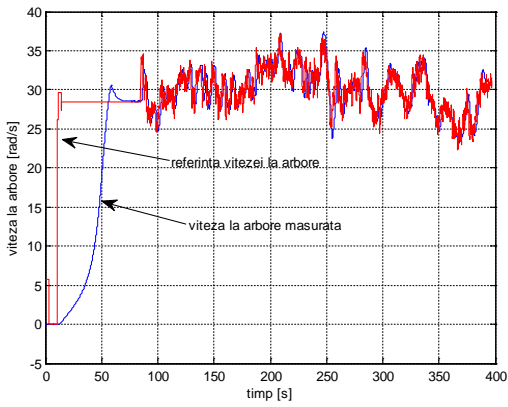




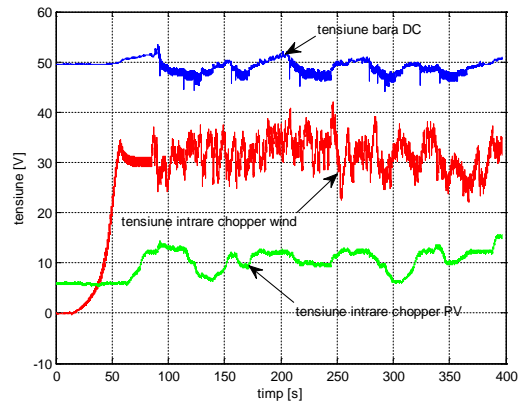
c)



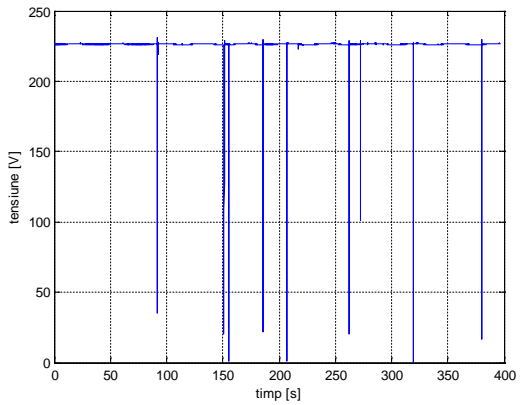
d)



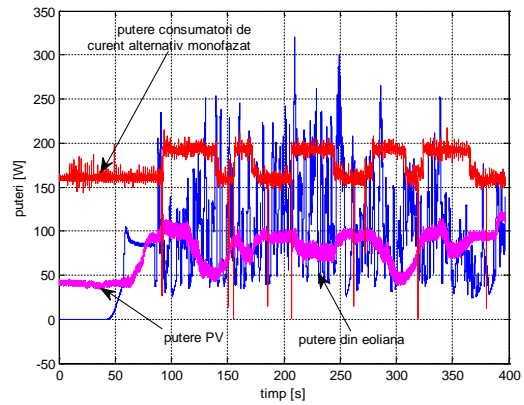
e)



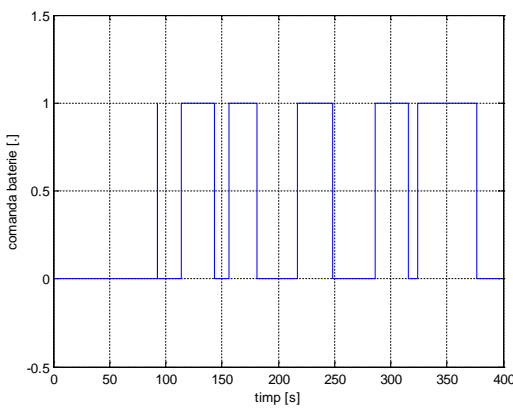
f)



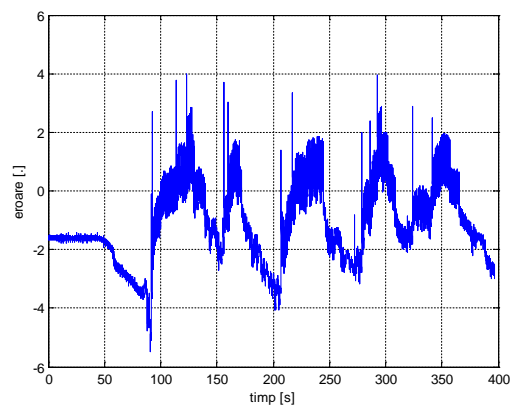
g)



h)



i)



j)

Fig. IV.2. Evolution of main features of the integrated energy production and use system when the two renewable sources supplies, the battery, the mono-phase AC consumers and the national grid are connected, with fuzzy controller

The evolution of input voltage at PV chopper and chopper wind simulator are shown in Figure IV.2f, along with voltage variation on the DC line. Figure IV.2g shows the evolution of

voltage for single-phase power supply to consumers, and Figure IV.2h shows the evolution of source powers and consumers.

When using the fuzzy controller, as can be noted in Figure IV.2j, the battery voltage adjustment is achieved to a satisfactory level. However, the setting error in this case is higher than in the previous case. Instead, Figure IV.2i shows a much smaller number of battery charge/discharge switches, which was consistent with the objective established for the upper-level hierarchical control senior of the integrated system. As a matter of fact, we believe this solution to be superior if we consider the mixed criterion of performance evaluation of a system of energy production and distribution.

Conclusions

The objectives set for 2017 have been fully achieved and **all the activities in the implementation plan have been carried out**. In the 2017 development stage, the results are as follows:

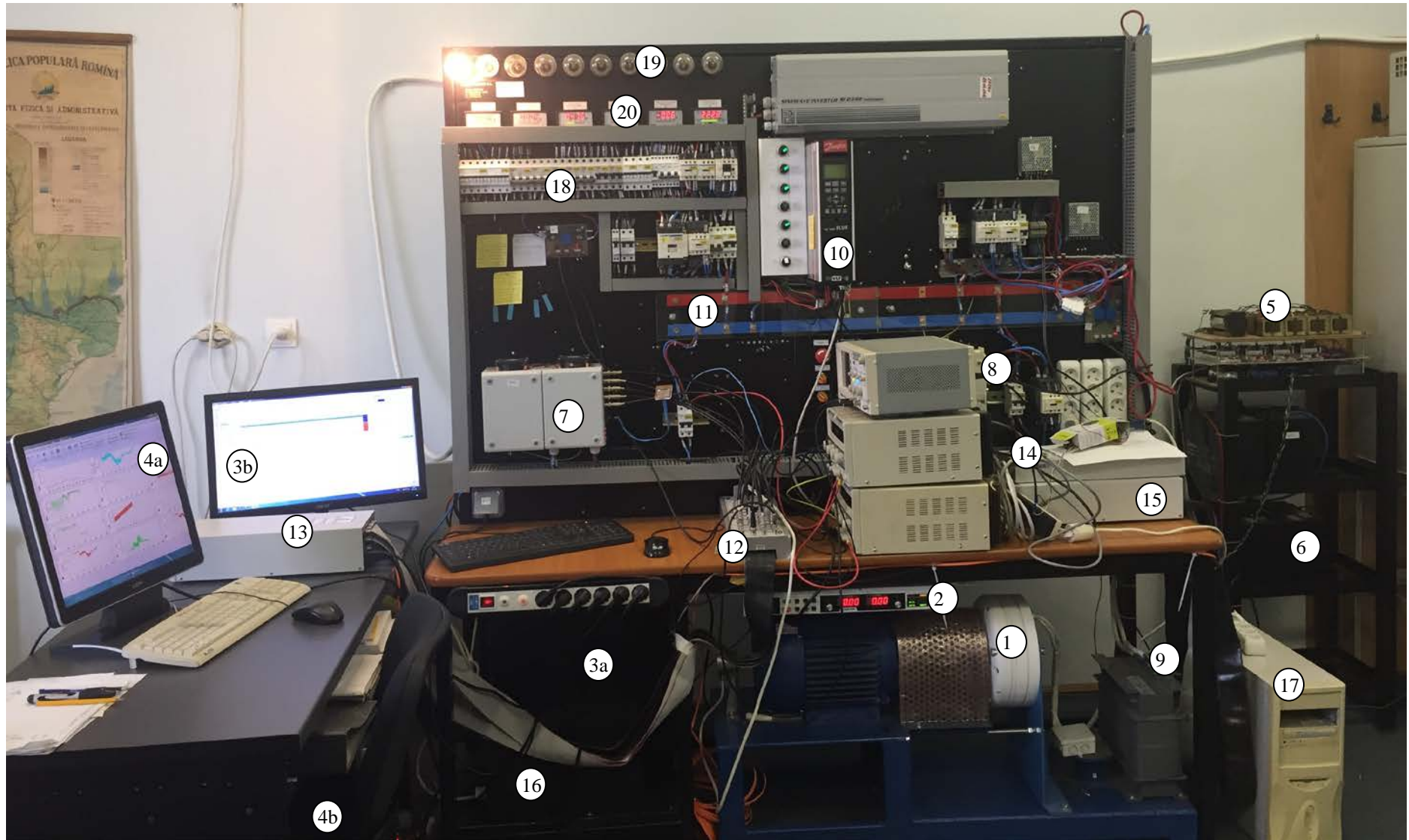
1. Scientific report (stage 2017);
2. Bidirectional converter for energy transfer to/from the grid;
3. Development system for the control of integrated energy production and use system;
4. Control structure and algorithms for the integrated system.

Dissemination of results

1. 4 scientific papers presented at BDI indexed conferences (IEEE Xplore) (all pending ISI Proceedings indexing);
2. a doctoral thesis for which the PhD title was confirmed by the minister of National Education (Order 4097 of June 20, 2017).

The physical achievements of the distributed system for electrical energy production and use are listed below:

1. electro-mechanical wind turbine simulator;
2. photovoltaic system emulator;
3. monitor and computer for upper-level control;
4. monitor and computer for lower level control;
5. inverter/active power filter (APF);
6. battery pack;
7. chopper for the photovoltaic emulator;
8. chopper for the wind turbine electro-mechanical simulator;
9. three-phase transformer for connection to the national grid;
10. Danfoss VLT 5000 frequency converter;
11. DC bus;
12. CP 1103 controller board-1;
13. PX4 box-1;
14. CP 1103 controller board -2;
15. PX4 box-2;
16. UPS;
17. AC consumer for inverter/APF;
18. distribution, control and protection circuits;
19. AC consumers;
20. panel devices.



Physical development of the setup for the intelligent hierarchical control of distributed systems of energy production and use